Impact of Spontaneous Synaptic Activity on the Resting Properties of Cat Neocortical Pyramidal Neurons In Vivo

DENIS PARÉ,[1] ERIC SHINK,[1] HÉLÈNE GAUDREAU,[1] ALAIN DESTEXHE,[1] AND ERIC J. LANG[2]
[1]*Département de Physiologie, Faculté de Médecine, Université Laval, Quebec, Quebec G1K 7P4, Canada; and*
[2]*Department of Physiology and Neuroscience, New York University Medical Center, New York, New York 10016*

Paré, Denis, Eric Shink, Hélène Gaudreau, Alain Destexhe, and Eric J. Lang. Impact of spontaneous synaptic activity on the resting properties of cat neocortical pyramidal neurons in vivo. *J. Neurophysiol.* 79: 1450–1460, 1998. The frequency of spontaneous synaptic events in vitro is probably lower than in vivo because of the reduced synaptic connectivity present in cortical slices and the lower temperature used during in vitro experiments. Because this reduction in background synaptic activity could modify the integrative properties of cortical neurons, we compared the impact of spontaneous synaptic events on the resting properties of intracellularly recorded pyramidal neurons in vivo and in vitro by blocking synaptic transmission with tetrodotoxin (TTX). The amount of synaptic activity was much lower in brain slices (at 34°C), as the standard deviation of the intracellular signal was 10–17 times lower in vitro than in vivo. Input resistances (R_{in}s) measured in vivo during relatively quiescent epochs (''control R_{in}s'') could be reduced by up to 70% during periods of intense spontaneous activity. Further, the control R_{in}s were increased by ~30–70% after TTX application in vivo, approaching in vitro values. In contrast, TTX produced negligible R_{in} changes in vitro (~4%). These results indicate that, compared with the in vitro situation, the background synaptic activity present in intact networks dramatically reduces the electrical compactness of cortical neurons and modifies their integrative properties. The impact of the spontaneous synaptic bombardment should be taken into account when extrapolating in vitro findings to the intact brain.

INTRODUCTION

The integrative properties of pyramidal neurons have received much attention lately (reviewed in Johnston et al. 1996; Yuste and Tank 1996). In these efforts, the brain slice maintained in vitro has been the preparation of choice because of recent developments in imaging and recording techniques. Even though it is commonly agreed that the integrative properties of pyramidal neurons might be quite different in vitro compared with in vivo, this point is commonly ignored when discussing the implications of in vitro findings for intact brains, probably because we lack quantitative estimates of the background synaptic activity affecting cortical neurons in vivo.

Yet, much evidence suggests that there are very important differences between the spontaneous synaptic activity present in these two preparations. Indeed, much of the synaptic connectivity is lost in brain slices and these experiments are often conducted at a low temperature. Moreover, each cortical pyramidal cell receives ~10,000 inputs (DeFelipe and Fariñas 1992), ~70% of which originate from other cortical neurons (Gruner et al. 1974; Szentágothai 1965). Considering that pyramidal cells were reported to fire at ~10 Hz in waking animals (Steriade 1978; Steriade et al. 1974) and because individual synaptic events produce transient increases in membrane conductance, it logically follows that background synaptic activity in the cortical network should have a major impact on the physiological properties of pyramidal neurons.

In agreement with this, biophysical simulations have revealed that network activity can dramatically reduce the input resistance (R_{in}) and time constant of neocortical pyramidal cells (Bernander et al. 1991). Moreover, it was consistently reported that cortical neurons have a lower R_{in} in vivo than in brain slices kept in vitro (see Bindman et al. 1988). Unfortunately, previous studies did not attempt to verify if the reduced level of spontaneous activity present in slices could account for the differences in R_{in}. Of course, factors other than differences in network activity might explain this. For instance, cellular penetration with sharp electrodes might cause more damage in vivo than in vitro because of differences in mechanical stability.

As the collective behavior of cellular ensembles is dependent on the computational properties of their individual components, resolving these issues is fundamental to understanding brain function. Further, such data are required to assess the implications of in vitro findings for the intact brain. Thus, we obtained quantitative estimates of this synaptic bombardment and of its impact on cortical neurons by studying the moment to moment variations in R_{in} induced by spontaneous synaptic events in neocortical pyramidal cells and by comparing their R_{in} before and after blocking synaptic transmission with tetrodotoxin (TTX) in vivo and in vitro. A preliminary version of this work has appeared in abstract form (Paré et al. 1997).

METHODS

Intracellular recordings in vivo

SURGERY. Experiments were conducted in agreement with ethics guidelines of the Canadian Council on Animal Care. Cats (2.5–3.5 kg) were anesthetized with pentobarbital sodium (Somnotol, 37 mg/kg ip) or with a ketamine-xylazine mixture (11 and 2 mg/kg im). Further, lidocaine (2%) was applied to all skin incisions and pressure points. The level of anesthesia was determined by continuously monitoring the electroencephalograph (EEG) contralateral to the intracellular recording site. Supplemental doses of Somnotol (5–7 mg/kg iv) or ketamine-xylazine (2 and 0.3 mg/kg, respectively, iv) were given to maintain a synchronized EEG pattern. Depending on the anesthetic, three to six supplemental doses were required during a typical 10–12 h experiment. The animals were paralyzed with gallamine triethiodide (33 mg/kg iv) and artificially ventilated only after the EEG displayed the usual pattern of deep general anesthesia. End tidal CO_2 concentration

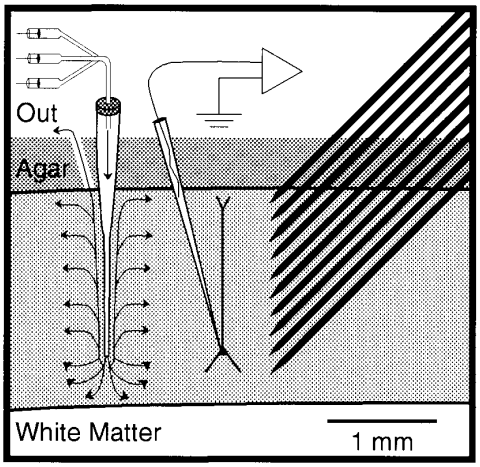

FIG. 1. Scheme of experimental set-up used for in vivo microinjection of tetrodotoxin (TTX). An array of 10 stimulating electrodes (*right*, dark lines) was inserted into center of gyrus at a 45° angle. To inject TTX, a micropipette (*left*) was inserted ~4 mm rostral to electrode array. Recording electrode (*middle*) was positioned halfway between the 2. Surface was covered with a layer of agar, except for a small outlet channel (out) created by leaving a pipette in place until agar hardened. A solution (Ringer or Ringer + TTX, 50 μM) was pumped continuously through injection pipette (1–1.5 μl/min) for duration of recording session. See METHODS for details.

was kept at 3.7 ± 0.2%, and the rectal temperature at 37–38°C with a heating pad. A lactated Ringer solution was administered (20 ml sc) twice during the experiment for fluid replacement.

To ensure recording stability, the cisterna magna was drained, the cat suspended, and a bilateral pneumothorax performed. The bone and dura overlying the suprasylvian gyrus (areas 5–7) were removed, and an electrode array, consisting of 10 fine tipped tungsten rods cemented together with a 150 μm intertip spacing, was inserted into the center of the gyrus at a 45° angle in the parasagittal plane (Fig. 1). These stimulating electrodes were used to evoke synaptic events and to insure that the block of spike-dependent synaptic events by TTX was complete and affected axons present in all cortical layers.

MICROPERFUSION OF TTX. An injection micropipette (75 μm tip diameter) was inserted ~4 mm rostral to the electrode array to a depth of 1.5 mm. The recording electrode was positioned halfway between the two and lowered 200 μm on a 20° angle with a piezoelectric manipulator. The surface was then covered with a layer of agar, except for a small outlet channel created by leaving a pipette in place until the agar hardened (Fig. 1). A solution (Ringer or Ringer + TTX, 50 μM) was pumped continuously through the pipette (1–1.5 μl/min) for the duration of the recording session; the dialyzing solution was changed with a liquid switch (BioAnalytical Systems, West Lafayette, IN). TTX was obtained from Sigma. The Ringer solution contained (in mM) 126 NaCl, 26 $NaHCO_3$, 3 KCl, 1.2 KH_2PO_4, 1.6 $MgSO_4$, 2 $CaCl_2$, 5 *N*-2-hydroxyethylpiperazine-*N*′-2-ethanesulfonic acid (HEPES), and 15 glucose.

RECORDING AND ANALYSIS PROCEDURES. EEG recordings were obtained using pairs of tungsten electrodes (0.5 MΩ) whose tips were separated by 1.5 mm in the vertical axis, with the superficial electrode located on the brain surface. Intracellular recordings were made using a high-impedance amplifier with active bridge circuitry. Typically, cells were recorded from for 30–120 min. Bridge balance was checked regularly during the recordings. The bridge was adjusted so that the onset and offset of the voltage responses to the intracellular current pulses were devoid of instantaneous resistive components. The intracellular and EEG signals were stored on tape. Analysis was performed off-line with the software IGOR (Wavemetrics, OR).

When testing the effect of TTX on the R_{in} of cortical neurons, intracellular current injection was used to maintain their V_m at approximately −70 to −75 mV (''manual clamp''), below the activation threshold of the persistent Na^+ current. The amplitude of this steady current was adjusted so that the V_m returned to a constant value during epochs that were relatively free of synaptic events. As TTX always produced a gradual hyperpolarization in vivo, this maneuver aimed at dissociating the effects of the synaptic blockade on the R_{in} from the voltage-dependent activation or inactivation of intrinsic currents that could have been produced by the hyperpolarization. In addition to the steady current injection, a brief (200–400 ms) hyperpolarizing current pulse of constant amplitude (0.1–0.4 nA) and an intracortical shock were applied at regular intervals (every 3–6 s) to monitor the R_{in} and the effect of TTX on spike-dependent synaptic transmission, respectively.

Unless otherwise stated, the standard deviation of the intracellular signal was measured from ~1 min epochs of spontaneous data obtained at a V_m of approximately −70 mV as determined by intracellular injection. The signal was sampled at 5 kHz (for a total of ~300,000 data points) and the positive phase of action potentials was digitally deleted. The values of these data points (usually 2) were replaced by that of points immediately preceding the action potentials. No attempt was made to delete spike afterpotentials because they were distorted by spontaneous synaptic events.

HISTOLOGY. Histological controls were performed to confirm the depth and morphology of the recorded cells. In many experiments, Neurobiotin was added to the electrolytic solution (1%) to identify the morphology of the recorded cells. The presence of Neurobiotin did not appear to alter the electrophysiological properties of the recorded neurons. We found that it is not necessary to pass large currents through the intracellular pipette to stain the cells, as Neurobiotin appeared to diffuse on its own throughout the cell during the course of our recordings. At the conclusion of the experiments, the animals were administered a lethal dose of pentobarbital and perfused with 500 ml of chilled saline (0.9%) followed by 1 L of a solution of 2% paraformaldehyde and 1% glutaraldehyde in 0.1 M phosphate buffered saline (PBS, pH 7.4). The brain was stored in 30% glucose solution overnight and then transferred to PBS. Sagittal sections (80 μm) were cut on a freezing microtome. Neurobiotin-filled cells were visualized by incubating the sections in the avidin-biotin-horseradish peroxidase (HRP) solution (ABC Elite Kit, Vector Labs) and processed to reveal the HRP staining (Horikawa and Armstrong 1988).

Intracellular recordings in vitro

Guinea pigs (Hartley, 250 g) and cats (2.5–3.5 kg) were deeply anesthetized (pentobarbital, 50 mg/kg ip). Then, guinea pigs were decapitated and their brains removed. In cats, an extensive craniotomy was performed before excising the suprasylvian gyrus. Cortical slices were sectioned on a vibrating microtome at a thickness of 400 μm. Slices were submerged and continuously perfused with a solution at 32–34°C containing (in mM) 126 NaCl, 3 KCl, 1.6 $MgSO_4$, 26 $NaHCO_3$, 1.25 NaH_2PO_4, 2 $CaCl_2$, and 10 glucose, saturated with 95% O_2-5% CO_2 to a final pH of 7.4. Recordings began at least 1 h after preparation of the slices. They were performed in the suprasylvian gyrus (areas 5–7) in cats and in the homologous cortical region of guinea pigs.

Because no significant differences were found between the V_m (guinea pig −78.6 ± 1.6 mV, $n = 14$; cat −80.1 ± 0.98 mV, $n = 9$; $t = 0.54$, $P < 0.59$, 2-tailed), spike amplitude (guinea pig 83.7 ± 1.15 mV; cat 83.4 ± 1.54 mV; $t = 0.14$, $P < 0.89$, 2-tailed), and R_{in} (guinea pig 67.24 ± 6.74 MΩ; cat 64.4 ± 5.37 MΩ; $t = 0.29$, $P < 0.77$, 2-tailed) of cat and guinea pig cortical neurons, the results obtained in these two species were combined.

RESULTS

Intracellular recordings of regular spiking (Connors et al. 1982; McCormick et al. 1985) neocortical neurons that had membrane potentials (V_m) > -60 mV and overshooting action potentials were obtained in anesthetized cats and from cat or guinea pig cortical slices kept in vitro. Fast-spiking neurons (Connors et al. 1982; McCormick et al. 1985) were not considered in this study. All intracellular recordings were obtained from the suprasylvian gyrus (areas 5–7) in cats and from the homologous region in guinea pigs. A total of 110 neurons were recorded in vivo and 39 in vitro (9 in cats and 30 in guinea pigs). All cells were recorded with KCl-filled pipettes (2.5 M; ~25 MΩ; tip diameter < 0.5 μm) pulled from the same batch of glass capillaries with identical puller settings. Moreover, to insure uniform electrode characteristics, no attempt was made to bevel or otherwise alter the shape of the pipette tips.

Ideally, the in vivo experiments should have been carried out in unanesthetized animals. However, because it is impossible to obtain stable intracellular recordings of long duration in unanesthetized animals, these experiments were performed under two different anesthetic conditions to insure that our conclusions were not critically dependent on the type of anesthetic. These anesthetics were pentobarbital, which potentiates γ-aminobutyric acid ($GABA_A$) synaptic events (Barker and McBurney 1979) and ketamine-xylazine, which blocks *N*-methyl-D-aspartate (NMDA)(Anis et al. 1983) and activates α2 noradrenergic receptors (Nicoll et al. 1990), respectively. Of the 110 neurons recorded in vivo, 63 were recorded under barbiturate anesthesia, and 47 under ketamine-xylazine. No attempt was made to control for differences in temperature between the in vivo and in vitro preparations, because we wanted to compare them as they are commonly used.

In several experiments, the morphology of the recorded cells was identified by intracellular injection of Neurobiotin (Fig. 2). All regular spiking neurons that were recovered (27 in vivo and 1 in vitro) had pyramidal morphological features including a dominant apical dendritic trunk, a conical cell body, and spiny dendrites. Most of these cells (79%) were located in infragranular layers. The sample of unlabeled in vivo cells contained a similar proportion of layer V-VI neurons based on their depths (75%). Similarly, the majority of in vitro neurons were infragranular cells as we aimed for deep cortical layers. Considering that anatomic studies have revealed that pyramidal neurons account for 70–85% of cortical cells (DeFelipe and Fariñas 1992) and because aspiny neurons were reported to have a very different firing pattern (McCormick et al. 1985), we are confident that most cells described here were pyramidal neurons.

Comparison between the spontaneous activity observed in vivo and in vitro

The most conspicuous difference between in vivo and in vitro recordings was the paucity of spontaneous synaptic events observed in vitro. Because this applied to both cat and guinea pig neurons recorded in vitro, the results obtained in these two species were combined. This is exemplified in Fig. 3 where the activity of regular spiking cortical neurons recorded at rest from infragranular layers in vivo (Fig. 3*A1*) and in vitro (at 34°C; Fig. 3*B1*) is shown with the same gain and time base. Whereas the in vivo recording displayed a continuous barrage of compound postsynaptic potentials (PSPs) that often summated into large (2–15 mV) events, the in vitro recording was characterized by long quiescent periods interrupted by brief bursts of small amplitude PSPs. Furthermore, spontaneous synaptic potentials often gave rise to action potentials in vivo (Fig. 3*A1*), but rarely did so in vitro (Fig. 3*B1*). An example of a high-frequency (~150 Hz) spike train triggered by spontaneous synaptic events that coincided with a depth negative EEG potential is shown with an expanded time base in Fig. 3*A3*. These differences were observed despite the fact that neurons recorded in vitro had much higher R_{in}s than those recorded in vivo (see below) and displayed normal responses to a graded series of current pulses (Fig. 3*B3*). To facilitate comparison between in vivo and in vitro data, epochs of spontaneous activity are depicted at a higher gain and faster time base in Fig. 3, *A4* and *B2*, respectively.

To quantify the difference in spontaneous synaptic activity between in vivo and in vitro recordings, we measured the standard deviation of the intracellular signal in neurons kept at around −70 mV with intracellular current injection. Subsets of 10 neurons were analyzed in each condition and action potentials were digitally deleted from the in vivo data. As shown in Fig. 3*C*, in vivo neurons recorded under ketamine-xylazine displayed the highest standard deviation, followed by those recorded under barbiturate. In neurons recorded in vitro, the standard deviation of the intracellular signal was 10 to 17 times lower, close to that of the equipment noise (0.18 ± 0.01 mV; $n = 3$) measured in the extracellular space after withdrawing the recording pipette from the cells. The differences between the standard deviation of the intracellular signal of neurons recorded in vitro and in vivo were statistically significant (in vitro vs. barbiturate, $t = 3.97$ $P < 0.005$; in vitro vs. ketamine-xylaxine, $t = 9.77$, $P < 0.001$, 2-tailed), as well as the differences observed in vivo between barbiturate and ketamine-xylazine anesthesia ($t = 2.53$, $P < 0.05$, 2-tailed). No differences were found between the standard deviation of the intracellular signal among cat and guinea pig cortical neurons recorded in vitro.

Influence of anesthetics on the spontaneous activity of cortical neurons in vivo

The difference between the standard deviation of the intracellular signal in neurons recorded in vivo under barbiturate or ketamine-xylazine anesthesia resulted from the strikingly dissimilar pattern of spontaneous activity induced by these anesthetics (compare Figs. 3*A* and 4*A*). In the posterior part of the suprasylvian gyrus, where most recordings were obtained, the intracellular activity observed under barbiturate anesthesia was characterized by large compound PSPs that recurred at ~2–3 Hz, in phase with depth-negative surface-positive EEG potentials (Fig. 3*A*). In Fig. 3*A1* for instance, note how the PSPs triggering action potentials generally coincided with depth-negative EEG potentials. DC hyperpolarization (Fig. 3*A2*) abolished most spikes and increased the amplitude of PSPs, but they still coincided with depth-negative EEG potentials.

A different pattern of spontaneous activity was observed under ketamine-xylazine anesthesia. In agreement with pre-

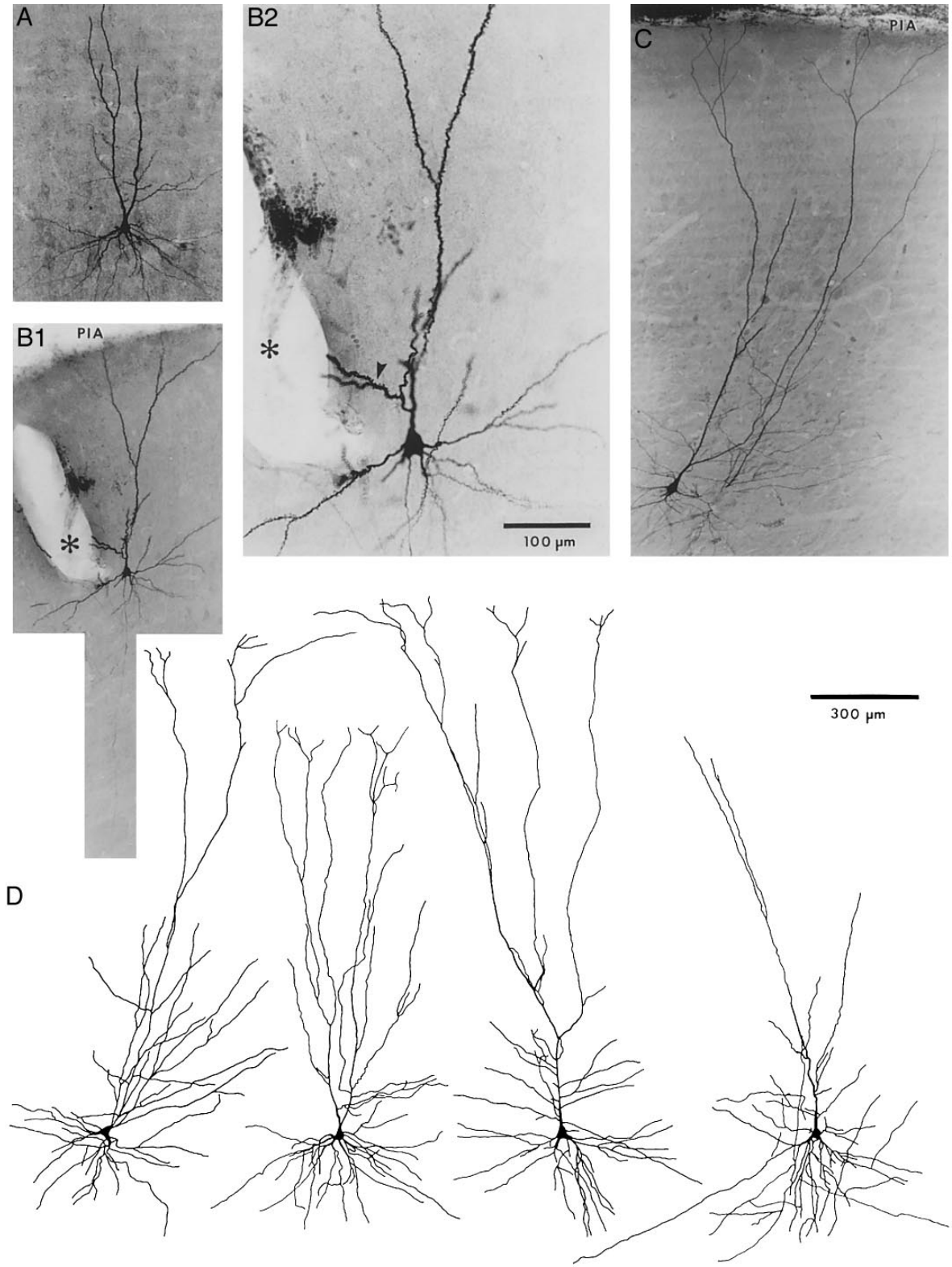

FIG. 2. Morphological identification of cortical neurons. *A–C*: photomicrographs of supragranular (*A* and *B*) and infragranular (*C*) pyramidal neurons morphologically identified by intracellular injection of Neurobiotin. *B*: ∗, a blood vessel and ▼, a spiny dendritic segment. *D*: reconstruction of 4 deep pyramidal neurons from 3–5 consecutive sections. Activity of 1st and 3rd cell from left is illustrated in Figs. 3*A* and 4, respectively. Calibration bar in *D* is valid for *A*, *B1*, and *C*.

vious findings (Steriade et al. 1993b), neurons recorded in this condition displayed a slow V_m oscillation at <1 Hz (Fig. 4). The depolarized phase of this oscillation coincided with depth-negative, surface-positive potentials in the local EEG and its hyperpolarized phase with depth-positive, surface-negative EEG potentials (Fig. 4*C*) (Contreras and Steriade

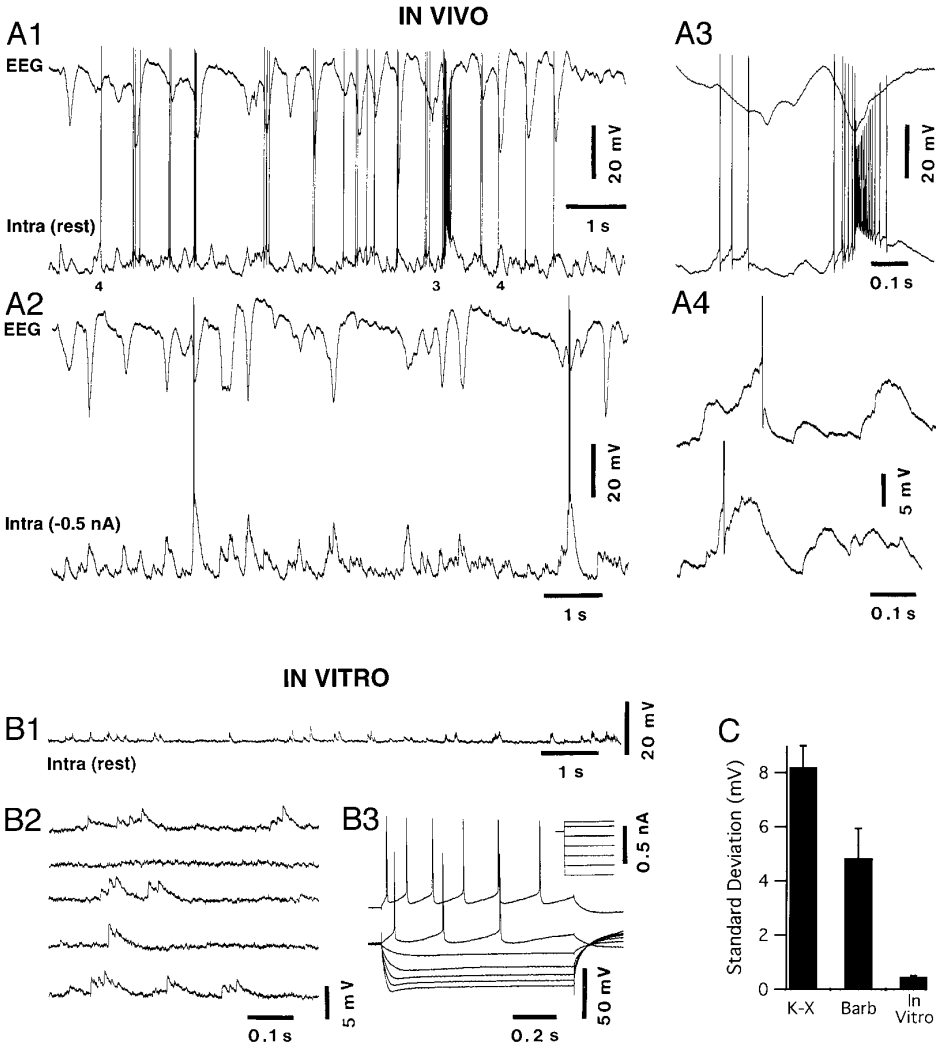

FIG. 3. Comparison of spontaneous synaptic activity displayed by cat neocortical neurons in vivo (*A*) and in vitro (*B*). *A*: intracellular recording (Intra) of an infragranular regular spiking cortical cell at rest (−64 mV; *A1*) and at −82 mV (*A2*) and simultaneously recorded electroencephalograph (EEG) under barbiturate anesthesia. Note large amplitude PSPs coinciding with depth negative EEG potentials. Intracellular events marked by numbers in *A1* are expanded in *A3* and *A4*. *B1*: intracellular recording (Intra) of an infragranular regular spiking cortical neuron at rest (−76 mV) recorded in a cat slice at 34°C. Same gain and time base as in *A1*. *B2*: spontaneous synaptic potentials at a higher gain (same as in *A4*). *B3*: response of same neuron to current pulses of various amplitudes. *C*: histogram comparing standard deviation of intracellular signal in vivo under ketamine-xylazine (K-X; $n = 10$) or barbiturate (Barb; $n = 10$) anesthesia as well as in vitro ($n = 10$).

1995). As shown in Fig. 4*B1* [expanded from the segment marked (∗) in Fig. 4*A*, *left*], the depolarized phase of the oscillation appeared to result from the summation of numerous PSPs. By contrast, a progressive decrease in the variability of the intracellular signal occurred during the hyperpolarization (cf. Fig. 4, *B2* and *B3*), consistent with a massive disfacilitation. Further, the two phases of the oscillation were differentially affected by the injection of intracellular current, the hyperpolarized phase being much more sensitive than the depolarized one (Fig. 4*A*). These observations suggest that the R_{in} was relatively increased during the hyperpolarized phase, in agreement with previous findings (Contreras et al. 1996).

In all neurons recorded in vivo under ketamine-xylazine, the two phases of the oscillation gave rise to bimodal distributions of V_m values. This is shown in Fig. 5*A* where we superimposed three V_m distributions computed from stationary epochs of one minute obtained at different degrees of membrane polarization in the same neuron (spontaneous spikes were deleted digitally). In each histogram, the first mode, at negative values, corresponds to the hyperpolarized phase of the slow oscillation whereas the second corresponds to its depolarized phase. These bimodal histograms translated into cumulative V_m distributions with a characteristic biphasic rise (Fig. 5*B*). Further, the differential effect of current injection on the two phases of the oscillation is manifested by the relatively invariant position of the depolarized mode compared with that of the hyperpolarized one (Fig. 5*A*) and by the gradually decreasing distance between the cumulative distributions from hyperpolarized to depolarized V_ms (Fig. 5*B*).

As the amount of spontaneous synaptic activity in vivo was constantly changing, inferring the R_{in}s of the recorded neurons from their voltage response to series of current pulses of increasing amplitude proved inadequate. Thus, to quantify the moment to moment changes in R_{in} associated with the varying level of spontaneous synaptic activity, a new statistical method was used. This method involved computing V_m distributions at various degrees of membrane polarization as determined by steady current injection during stationary epochs (~1 min) of spontaneous activity (Figs. 5*A* and 6*A*). Action potentials were digitally deleted to insure comparability of V_m distributions observed at different degrees of polarization (see METHODS). Further, neurons displaying marked inward rectification in the hyperpolarizing direction were not considered for this analysis. In neurons recorded in vivo, these distributions were markedly skewed to the right and the level of positive skew increased with membrane hyperpolarization. It should be pointed out that with KCl-filled pipettes, the vast majority of synaptic

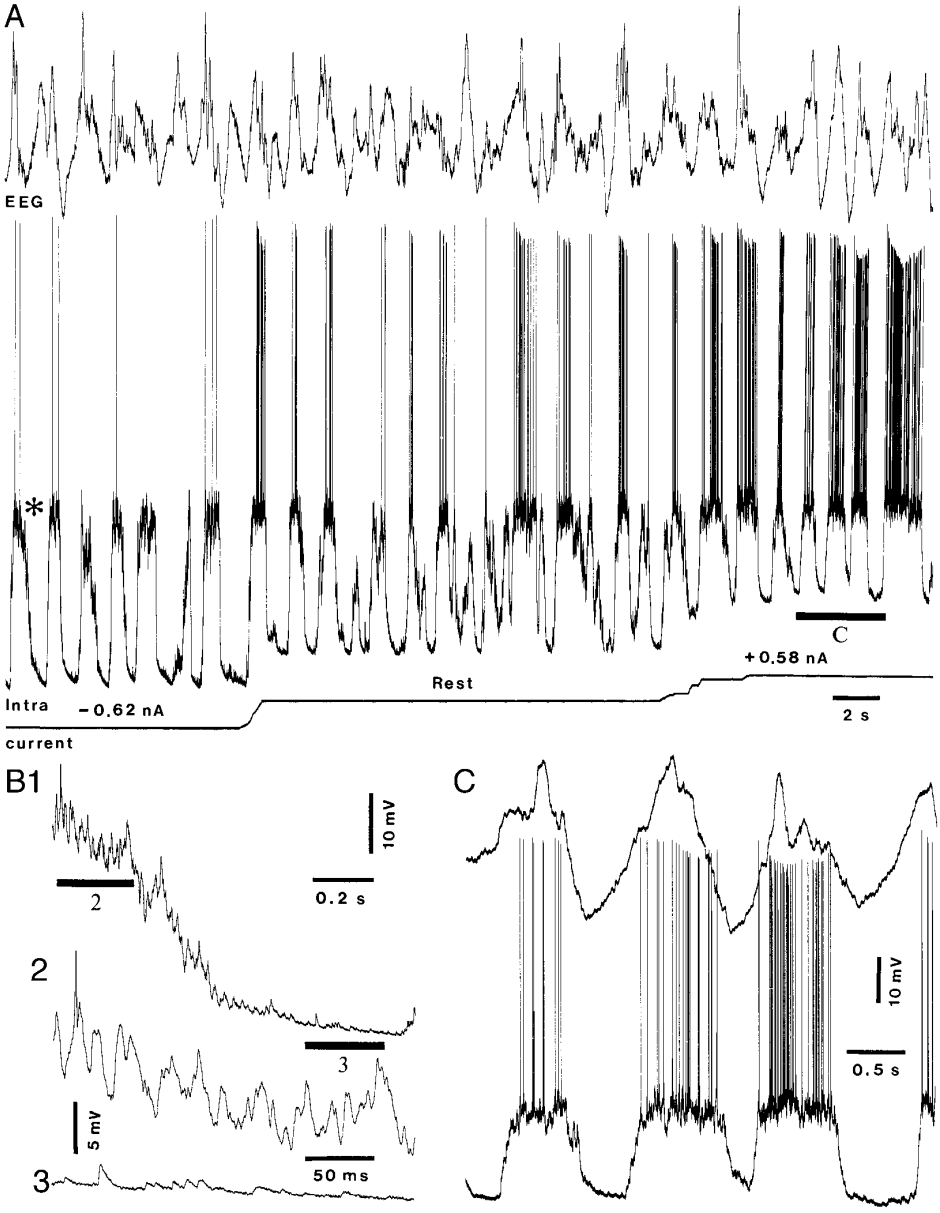

FIG. 4. Spontaneous synaptic activity under ketamine-xylazine anesthesia. *A*: simultaneous surface cortical EEG and intracellular recording (Intra) of a deep pyramidal neuron. This neuron was recorded at various V_ms as determined by different amounts of intracellular current injection. Intracellular event (∗) in *A* (*left*) is shown at higher gains in *B*. Intracellular events marked by *C* in *A* are shown with an expanded time base in *C*. Note slow V_m oscillation in phase with cortical EEG.

events are depolarizing so that more depolarized V_ms should reflect higher levels of spontaneous synaptic activity associated with lower R_{in}s. Moreover, as the V_m distributions were computed from long epochs of spontaneous activity, the V_m values observed at the same percentile in the different distributions should reflect a similar level of spontaneous synaptic bombardment. Consequently, by plotting V_m values as a function of injected current at various cutoff percentiles in the V_m distributions, we could estimate, from the slope of the fitted curves, the R_{in}s of recorded neurons at different intensities of synaptic bombardment (see Figs. 5 and 6).

To quantify the changes in R_{in} occurring in relation to the slow ketamine-xylazine oscillation, we plotted V_m values at various percentiles in the cumulative distributions as a function of injected current and estimated the R_{in} from the slope of the fitted curve (Fig. 5*C*). The bottom curve (Fig. 5*C*, ■) was constructed from the V_m values of the first mode in the V_m histograms (~20% in cumulative distributions). Curve-fitting with the least-squares method yielded a R_{in} of 16 MΩ. As the curves were plotted from voltages obtained at progressively higher percentiles in the cumulative distributions, the slope of the fitted curve diminished indicating gradually decreasing R_{in}s (from 16 mΩ at 20% to 4 MΩ at 95%). Similar results were obtained in other neurons where V_m distributions were constructed from epochs of spontaneous activity obtained with various degrees of membrane depolarization *or* hyperpolarization provided that less than ±0.7 nA was injected. Thus it appears that the R_{in} drops observed at more depolarized cutoff percentiles reflect the effect of spontaneous synaptic activity rather than that of voltage-dependent rectification.

It is important to emphasize that this method does not take into account the fact that the distance between the recording site and the active synapses might vary. However, as the impact of electrotonically remote synaptic events diminishes with distance from the recording site and because there is no reason to assume that inputs ending at distinct electrotonic distances are recruited at different times in the

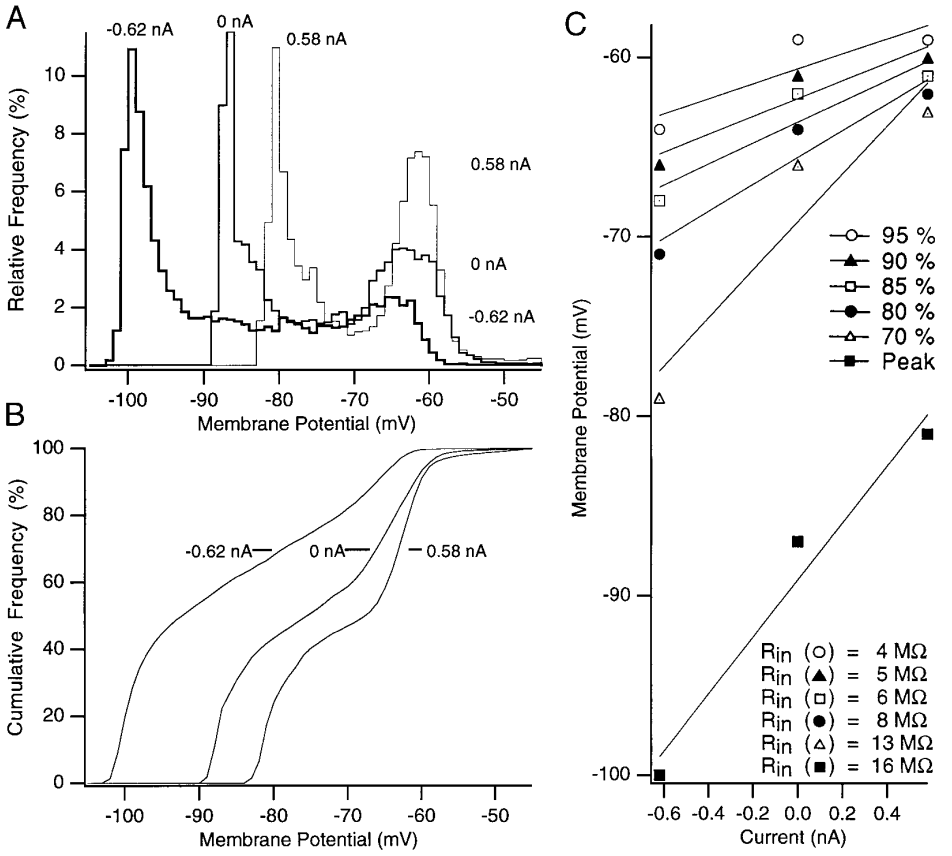

FIG. 5. Effect of membrane polarization on distribution of membrane potentials in a deep pyramidal neuron recorded under ketamine-xylazine anesthesia. *A*: 3 superimposed normalized histograms of V_m values computed from 1-min epochs sampled at 5,000 Hz. Action potentials were deleted digitally. Note bimodal distribution and differential effect of current injection on 2 modes. With −0.62, 0, and 0.58 nA, left-hand side modes were −100, −88, and −81 mV, and averages were −86.3 ± 13.5 mV, −74.1 ± 10.9 mV, and −69.2 ± 9.1 mV, respectively. *B*: cumulative histogram of V_m values computed from same data. *C*: plots of membrane potential below which 70, 80, 85, 90, and 95% of values are found as a function of injected current. Lowest curve (■) was constructed with V_m of mode. R_{in}s were estimated from slope of fitted curve (least-squares method).

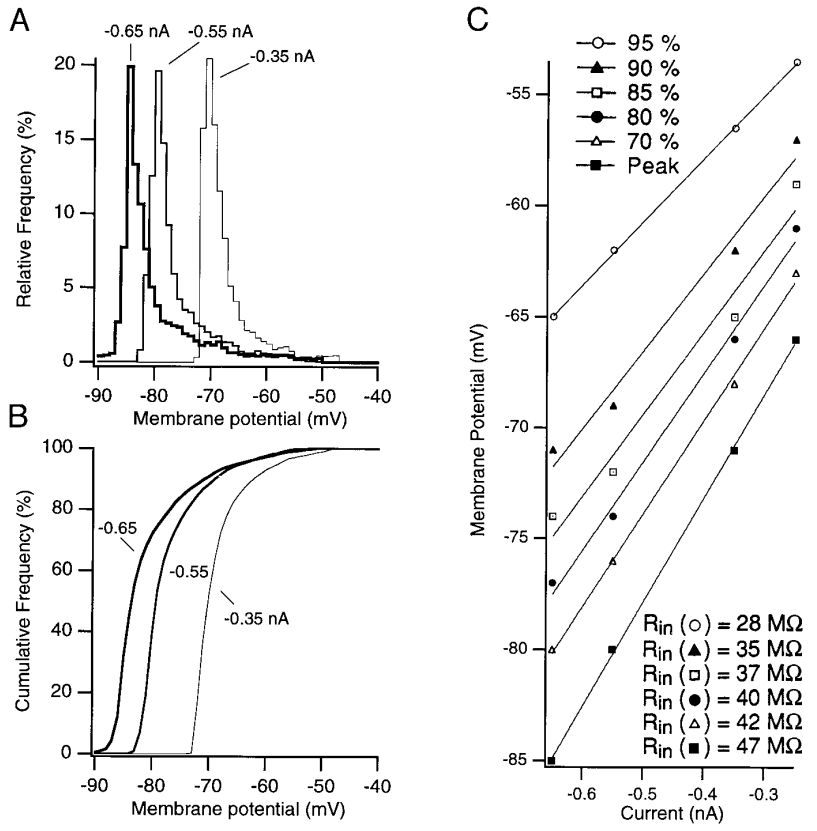

FIG. 6. Effect of membrane polarization on distribution of membrane potentials in a deep pyramidal neuron recorded under barbiturate anesthesia. *A*: 3 normalized histograms of V_m values during 1-min epochs where cell was injected with different amounts of current. See Fig. 5 for technical details. With −0.65, −0.55, and −0.35 nA, left-hand side modes were −85, −80, and −71 mV and averages were −79.9 ± 7.03 mV, −76.1 ± 5.69 mV, and −67.6 ± 4.69 mV, respectively. *B*: cumulative histogram of V_m values computed from same data. *C*: plots of membrane potential below which 70, 80, 85, 90, and 95% of values are found as a function of injected current. Lowest curve (■) was constructed with V_m of mode. R_{in}s were derived from slope of fitted curve (least-squares method).

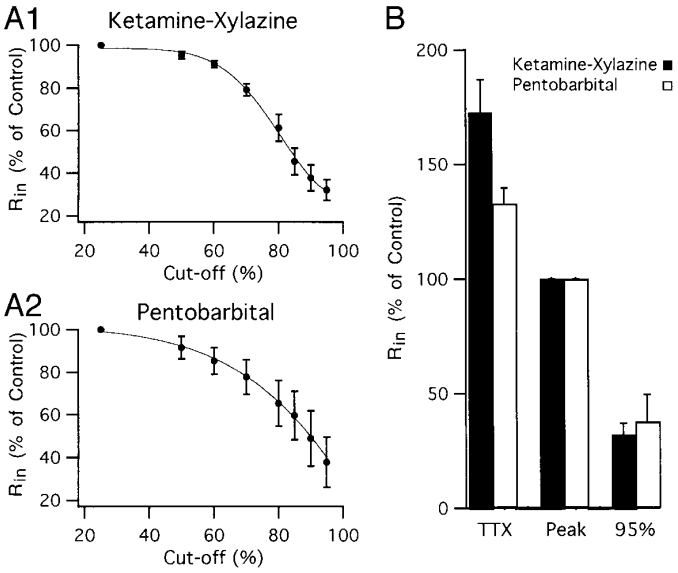

FIG. 7. Impact of spontaneous synaptic events on R_{in} of pyramidal neurons under ketamine-xylazine and barbiturate anesthesia. *A*: normalized plots of change in R_{in} as a function of percent cutoff used to analyze effects of membrane polarization on V_m distributions (see Figs. 5 and 6) under ketamine-xylazine (*A1*) and barbiturate (*A2*) anesthesia. *B*: histogram comparing effect of TTX and synaptic activity on R_{in} of pyramidal neurons recorded under ketamine-xylazine (solid bars) and barbiturate anesthesia (empty bars). Data normalized to ''control'' R_{in} estimated from current-voltage plots of peak value of membrane potential distributions under various degrees of membrane polarization.

depolarizing phase, this factor probably has a minor impact on our R_{in} estimates.

Similar analyses were carried out on neocortical cells recorded under barbiturate anesthesia (Fig. 6). In keeping with the fact that the intracellular activity was less regular under barbiturate anesthesia, V_m distributions were never bimodal under barbiturate but displayed increasing degrees of positive skew at more hyperpolarized V_ms (Fig. 6*A*). Further, cumulative distributions rose monotonically (Fig. 6*B*) thus contrasting with the biphasic rise characterizing ketamine-xylazine recordings. However, as was observed under ketamine-xylazine, the distance between the cumulative V_m distributions obtained at various levels of polarization gradually diminished from hyperpolarized to depolarized V_ms. Consistent with this, plotting V_m values at progressively higher percentiles in the cumulative distributions as a function of injected current revealed a gradual decrease in R_{in} with increasing amounts of synaptic activity. In the example of Fig. 6*C* for instance, the R_{in} decreased from 47 MΩ at the histogram peak (~20–30%) to 28 MΩ at 95%.

Figure 7*A* summarizes the fluctuations in R_{in} estimated in cortical neurons recorded under ketamine-xylazine (Fig. 7*A1*; $n = 10$) or barbiturate anesthesia (Fig. 7*A2*; $n = 10$). For comparison purposes, the R_{in}s estimated at different percentiles in the cumulative distributions were normalized to those based on the V_m values of the histogram peaks. Hereafter, this R_{in} will be termed control R_{in}. However, it will be shown later that although this control R_{in} reflects a relatively quiescent state in the cortical network, it is still substantially reduced by spontaneous synaptic events. As illustrated in Fig. 7*A*, spontaneous synaptic activity significantly reduced the apparent R_{in} down to 32 and 38% of control R_{in}s under ketamine-xylazine ($t = 11.98$, $P < 0.001$, 2-tailed) and barbiturate ($t = 4.85$, $P < 0.001$, 2-tailed) anesthesia, respectively. These R_{in} decrements were measured using V_m values corresponding the 95th percentile of the cumulative V_m distributions.

Comparison between the resting properties of neocortical cells in vivo and in vitro

To further characterize the differences between in vivo and in vitro recordings, we compared the resting V_m and R_{in} of cortical neurons recorded in these two conditions. As there is no really quiescent state in vivo, resting V_m was defined here as the V_m value measured at the peak of frequency distributions obtained in periods free of DC current injection. Similarly, in vivo R_{in}s were estimated from their voltage responses to small hyperpolarizing pulses that were not obviously distorted by large synaptic events. For in vitro neurons where there was much less spontaneous activity, it was possible to plot their voltage responses to series of subthreshold current pulses of increasing amplitude and to estimate their R_{in} in the linear portion of the curve. Their resting V_m was measured in epochs devoid of synaptic activity.

By using this approach, it was determined that cortical neurons recorded in vitro had significantly higher R_{in}s (66.14 ± 1.3 MΩ; $n = 23$) than cells recorded in vivo under barbiturate (37.3 ± 3.9 MΩ; $n = 30$; $t = 4.82$, $P < 0.001$, 2-tailed) or ketamine-xylazine anesthesia (28.6 ± 4.2 MΩ; $n = 26$; $t = 6.08$, $P < 0.001$, 2-tailed). The V_m of neurons recorded in vitro (−79.2 ± 1.3 mV; $n = 23$) was more negative than that of cells studied in vivo under barbiturate (−66.9 ± 0.9 mV) or ketamine-xylazine anesthesia (−75.5 ± 2.7 mV). The V_m of neurons recorded under barbiturate was significantly more depolarized than that of neurons recorded in the other conditions (in vitro, $t = 7.78$, $P < 0.001$; ketamine-xylazine, $t = 3.02$, $P < 0.02$, 2-tailed). Moreover, the spike amplitude of neurons recorded in vitro (83.6 ± 1.92 mV, $n = 23$) was significantly higher than that of neurons recorded in vivo (68 ± 1.09 mV, $n = 33$, $t = 7.07$, $P < 0.001$, 2-tailed).

Effect of TTX on the resting properties of neurons recorded in vivo and in vitro

In keeping with the low standard deviation of the intracellular signal observed in vitro, bath application of TTX (1 μM) produced small but significant increases in R_{in} (4 ± 1.5%, $n = 7$, $t = 2.67$, $P < 0.05$, 2-tailed) provided that it was estimated from voltage responses to current pulses outside the region of inward rectification that characterizes these cells in the depolarized direction (Connors et al. 1982; Stafstrom et al. 1982). In contrast, in vivo dialysis of TTX produced large increases in R_{in} that averaged 72.8 ± 14.3% ($n = 11$) and 32.9 ± 6.8% ($n = 8$) of ''control'' values under ketamine-xylazine ($t = 5.09$, $P < 0.001$, 2-tailed) and barbiturate ($t = 4.84$, $P < 0.002$, 2-tailed) anesthesia, respectively. Further, the difference between the effect of TTX under ketamine-xylazine and barbiturate anesthesia was statistically significant ($t = 2.52$, $P < 0.05$, 2-tailed). These increases in R_{in} were paralleled by a significant membrane hyperpolarization of 7.8 ± 1.9 mV ($t = 4.1$, $P < 0.005$, 2-tailed) and 4.0 ± 1.1 mV ($t = 3.64$, $P < 0.01$, 2-tailed), respectively.

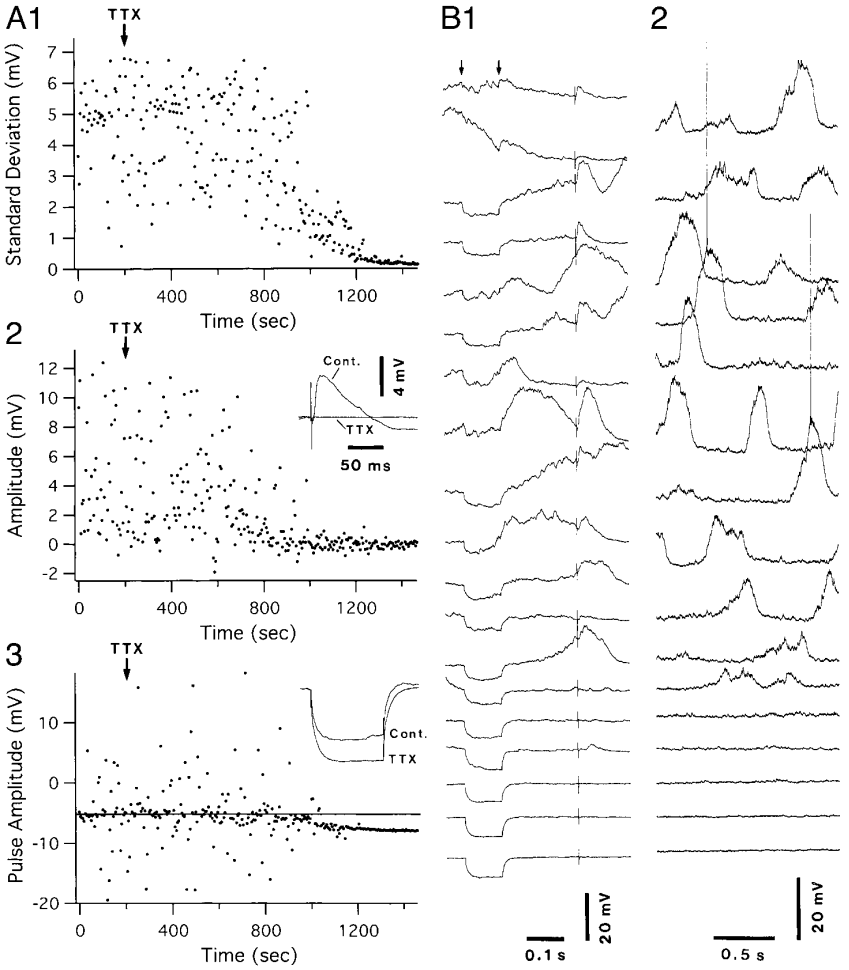

FIG. 8. Effect of TTX dialysis on R_{in} of an infragranular regular spiking cell. Graphs in *A* plot, as a function of time, standard deviation of intracellular signal (*A1*), amplitude of response to a cortical shock (*A2*), and voltage response to a current pulse of constant amplitude (0.2 nA; *A3*). ↓, onset of TTX dialysis. Standard deviation of intracellular signal was measured every 5 s, from stimulation-free epochs of 2 s. *A*, *2* and *3*, *insets*: comparison of cortically evoked response and voltage response to current pulses before and 20 min after onset of TTX dialysis. Averages of 20 sweeps, same scaling. *B*: samples of evoked (*B1*) and spontaneous (*B2*) intracellular events at regular intervals (1–1.5 min) during course of experiment.

Figure 1 illustrates the experimental approach used for in vivo dialysis of TTX. An example of such a test, carried out in a ketamine-xylazine anesthetized cat, is shown in Fig. 8. Initially, a continuous flow of Ringer solution (1.0 μl/min) was applied though the ejection pipette. A current pulse of constant amplitude followed by a subthreshold intracortical stimulus was applied every 3–6 s while manually clamping the cell so that the V_m returned to around −75 mV during the hyperpolarized phase of the slow oscillation (see METHODS). Figure 8*B* illustrates samples of evoked (Fig. 8*B1*) and spontaneous (Fig. 8*B2*) intracellular events at regular intervals (1–1.5 min) during the course of the experiment. After obtaining a baseline period, we switched the Ringer solution to one containing TTX (50 μM). Before the diffusion of the TTX, the pulse amplitude was highly variable as spontaneous synaptic events sometimes obliterated the response to the current pulse. TTX produced a gradual decline in standard deviation of the intracellular signal (Fig. 8*A1*) accompanied by a reduction in the amplitude of orthodromic responses (Fig. 8*A2*) and a 54% increase in the amplitude of the voltage response to the current pulses (Fig. 8*A3*). To determine whether these changes were statistically significant, we compared the preinjection period to an epoch of identical duration after TTX diffusion (40 data points or 200 s in each condition). For each parameter, the differences between the two conditions were found to be statistically significant (standard deviation, $t = 21.25$, $P < 0.001$; evoked response amplitude, $t = 7.48$, $P < 0.001$; pulse amplitude, $t = 3.9$, $P < 0.001$, 2-tailed).

Figure 7*B* puts these effects of TTX in the context of the moment to moment changes in R_{in} produced by fluctuations in network activity. In this case, we normalized the R_{in} changes induced by TTX and spontaneous network activities to the control R_{in}s measured during relatively ''quiet'' epochs. Such a graph thus documents the extreme variations in R_{in} that can be induced by spontaneous synaptic activity depending on the functional state of the network.

DISCUSSION

In this study, we estimated the impact of spontaneous synaptic activity on the resting properties of neocortical pyramidal neurons in vivo. By comparing V_m distributions obtained at different degrees of membrane polarization, we showed how the R_{in} of cortical cells in vivo varies from moment to moment, depending on the intensity of ongoing synaptic activity. Such analyses revealed that during epochs of intense synaptic bombardment, their R_{in} can be reduced by up to 70% relative to that estimated during periods that were free of large synaptic events. Further, even in this ''resting'' state, the R_{in} of cortical neurons is reduced by synaptic activity as TTX could increase their R_{in} by 30–70%. In contrast, spontaneous synaptic events were rare in cortical neurons recorded in vitro and bath application of TTX produced negligible increases in R_{in}.

It should be noted that the methods used here to estimate the changes in R_{in} do not distinguish the direct effects of synaptic inputs from their indirect effects on intrinsic membrane conductances. Indeed, the depolarization caused by the synaptic bombardment probably activated various inward and outward voltage-dependent conductances that reduced the R_{in}. However, even if these changes in membrane conductance are not caused directly by synaptic events, they remain an integral part of the impact of spontaneous synaptic activity on cortical cells.

Another factor that should be considered is that because we used sharp electrodes, the impact of synaptic events was probably underestimated. Indeed, the mechanical damage produced by the impalement with sharp electrodes has been shown to introduce a somatic shunt (Spruston and Johnston 1992). By reducing the R_{in}, this shunt probably decreased the influence of electrotonically remote synaptic events on our measurements thus leading us to underestimate the magnitude of R_{in} decrements produced by spontaneous network activities.

Similarly, it should be kept in mind that TTX application in vivo did not only abolish fast GABAergic and glutamatergic synaptic events but also suppressed modulatory inputs. Many modulatory actions (McCormick 1992), such as those of acetylcholine through muscarinic receptors (McCormick and Prince 1986) or those of glutamate through metabotropic receptors (Charpak et al. 1990), increase the R_{in} of cortical neurons. Thus, suppression of these effects by TTX probably led us to further underestimate the impact of fast synaptic events on the R_{in} of cortical neurons.

Nevertheless, the results of the present study suggest that differences in background synaptic activity account for a large portion of R_{in} differences between in vivo and in vitro recordings. Indeed, correcting control R_{in}s for the impact of the synaptic noise documented by in vivo applications of TTX revealed that background synaptic activities account for ~40–53% of R_{in} differences between in vivo and in vitro recordings. It would be premature to conclude that the remaining differences in R_{in} are due to the fact that sharp electrodes produce more damage in vivo than in vitro. First, pentobarbital directly activates $GABA_A$ receptors (Rho et al. 1996), whereas xylazine hyperpolarizes mammalian neurons by the activation of a potassium conductance through $\alpha 2$ noradrenergic receptors (Nicoll et al. 1990), thus reducing the R_{in} of in vivo neurons. Second, spike-independent synaptic events are more frequent in vivo than in vitro and produce significant R_{in} reductions in neocortical pyramidal cells (Paré et al. 1997).

It could be argued that the large impact of synaptic events documented in this study is an artifact induced by the anesthetics and that the background synaptic activity is much lower in conscious animals. However, this is inconsistent with the high rate of spontaneous discharge reported for corticofugal pyramidal neurons in unanesthetized animals (Steriade 1978; Steriade et al. 1974) and with the depressant actions of anesthetics on mammalian neurons. Moreover, under ketamine-xylazine anesthesia, electrical stimulation of brain stem activating systems that are believed to maintain the awake state in normal circumstances abolishes the hyperpolarized phase of the slow oscillation and maintains cortical cells in the depolarized phase (Steriade et al. 1993a). Thus, in this model of the waking state, cortical cells are kept at depolarized levels where their R_{in} is lowest.

These considerations thus suggest that the cortical network is constantly humming in conscious animals and that this produces dramatic reductions in the electrical compactness of cortical neurons. As this is likely to modify the integrative properties of pyramidal neurons, future modeling studies should aim at characterizing how the synaptic bombardment affects the interaction between synaptic inputs and active membrane properties in the dendrites of neocortical pyramidal neurons. Preliminary simulations (Destexhe and Paré 1997) suggest that the intense synaptic bombardment present in vivo tends to subdivide the dendritic tree of pyramidal neurons into localized regions that, to some extent, process synaptic inputs independently.

We thank M. Steriade for comments on an earlier version of this manuscript, as well as P. Giguère, E. Lebel, D. Drolet, and G. Oakson for technical and programming support.

This work was supported by grants from the National Sciences and Engineering Research Council, the Medical Research Council, and the National Institute of Neurological Disorders and Stroke.

Address for reprint requests: D. Paré, Dépt. de Physiologie, Faculté de Médecine, Université Laval, Québec City, Quebec G1K 7P4, Canada.

Received 15 July 1997; accepted in final form 14 November 1997.

REFERENCES

ANIS, N. A., BERRY, S. C., BURTON, N. R., AND LODGE, D. The dissociative anaesthetics, ketamine and phencyclidine, selectively reduce excitation of central mammalian neurones by *N*-methyl-D-aspartate. *Br. J. Pharmacol.* 79: 565–575, 1983.

BARKER, J. L. AND MCBURNEY, R. M. Pentobarbitone modulation of postsynaptic GABA receptor function on cultured mammalian neurones. *Proc. R. Soc. Lond. B Biol. Sci.* 206: 319–327, 1979.

BERNANDER, Ö., DOUGLAS, R. J., MARTIN, K. C., AND KOCH, C. Synaptic background activity influences spatiotemporal integration in single pyramidal cells. *Proc. Natl. Acad. Sci. USA* 88: 11569–11573, 1991.

BINDMAN, L. J., MEYER, T., AND PRINCE, C. A. Comparison of the electrical properties of neocortical neurons in slices in vitro and in the anaesthetized rat. *Exp. Brain Res.* 69: 489–496, 1988.

CHARPAK, S., GÄHWILER, B. H., DO, K., AND KNÖPFEL, T. Potassium conductances in hippocampal neurons blocked by excitatory amino-acid transmitters. *Nature* 347: 765–767, 1990.

CONNORS, B. W., GUTNICK, M. J., AND PRINCE, D. A. Electrophysiological properties of neocortical neurons in vitro. *J. Neurophysiol.* 48: 1302–1320, 1982.

CONTRERAS, D. AND STERIADE, M. Cellular basis of EEG slow rhythms: a study of dynamic corticothalamic relationships. *J. Neurosci.* 15: 604–622, 1995.

CONTRERAS, D., TIMOFEEV, I., AND STERIADE, M. Mechanisms of long lasting hyperpolarizations underlying slow sleep oscillations in cat corticothalamic networks. *J. Physiol. (Lond.)* 494: 251–264, 1996.

DEFELIPE, J. AND FARIÑAS, I. The pyramidal neuron of the cerebral cortex: morphological and chemical characteristics of the synaptic inputs. *Prog. Neurobiol.* 39: 563–607, 1992.

DESTEXHE, A. AND PARÉ, D. Spontaneous synaptic activity modulate action potential generation in neocortical pyramidal cells in vivo. *Soc. Neurosci. Abstr.* 23: 448, 1997.

GRUNER, J. E., HIRSCH, J. C., AND SOTELO, C. Ultrastructural features of the isolated suprasylvian gyrus. *J. Comp. Neurol.* 154: 1–27, 1974.

HORIKAWA, K. AND ARMSTRONG, W. E. A versatile means of intracellular labeling: injection of biocytin and its detection with avidin conjugates. *J. Neurosci. Methods* 25: 1–11, 1988.

JOHNSTON, D., MAGEE, J. C., COLBERT, C. M., AND CHRISTIE, B. R. Active properties of neuronal dendrites. *Annu. Rev. Neurosci.* 19: 165–186, 1996.

MCCORMICK, D. A. Neurotransmitter actions in the thalamus and cerebral cortex and their role in neuromodulation of thalamocortical activity. *Prog. Neurobiol.* 39: 337–388, 1992.

MCCORMICK, D. A. AND PRINCE, D. A. Mechanisms of action of acetylcho-

line in the guinea-pig cerebral cortex in vitro. *J. Physiol. (Lond.)* 375: 169–194, 1986.

MCCORMICK, D. A., CONNORS, B. W., LIGHTALL, J. W., AND PRINCE, D. A. Comparative electrophysiology of pyramidal and sparsely spiny stellate neurons of the neocortex. *J. Neurophysiol.* 54: 782–806, 1985.

NICOLL, R. A., MALENKA, R. C., AND KAUER, J. Functional comparison of neurotransmitter receptor subtypes in mammalian central nervous system. *Physiol. Rev.* 70: 513–565, 1990.

PARÉ, D., LEBEL, E., AND LANG, E. J. Differential impact of miniature synaptic potentials on the soma and dendrites of pyramidal neurons in vivo. *J. Neurophysiol.* 78: 1735–1739, 1997.

PARÉ, D., SHINK, E., GAUDREAU, H., DESTEXHE, A., AND LANG, E. J. Impact of spontaneous synaptic activity on the resting properties of neocortical pyramidal neurons in vivo. *Soc. Neurosci. Abstr.* 23: 448, 1997.

RHO, J. M., DONEVAN, S. D., ROGAWSKI, M. A. Direct activation of $GABA_A$ receptors by barbiturates in cultured rat hippocampal neurons. *J. Physiol. (Lond.)* 497: 509–522, 1996.

SPRUSTON, N. AND JOHNSTON, D. Perforated patch-clamp analysis of the passive membrane properties of three classes of hippocampal neurons. *J. Neurophysiol.* 67: 508–529, 1992.

STAFSTROM, C. E., SCHWINDT, P. C., AND CRILL, W. E. Negative slope conductance due to a persistent sodium current in cat neocortical neurons in vitro. *Brain Res.* 236: 221–226, 1982.

STERIADE, M. Cortical long-axoned cells and putative interneurons during the sleep-waking cycle. *Behav. Brain Sci.* 3: 465–514, 1978.

STERIADE, M., AMZICA, F., AND NUÑEZ, A. Cholinergic and noradrenergic modulation of the slow ($\approx$0.3 Hz) oscillation in neocortical cells. *J. Neurophysiol.* 70: 1385–1400, 1993a.

STERIADE, M., DESCHÊNES, M., AND OAKSON, G. Inhibitory processes and interneuronal apparatus in motor cortex during sleep and waking. I. Background firing and responsiveness of pyramidal tract neurons and interneurons. *J. Neurophysiol.* 37: 1065–1092, 1974.

STERIADE, M., NUNEZ, A., AND AMZICA, F. Intracellular analysis of relations between the slow ($<$1 Hz) neocortical oscillation and other sleep rhythms of the electroencephalogram. *J. Neurosci.* 13: 3266–3283, 1993b.

SZENTÁGOTHAI, J. The use of degeneration in the investigation of short neuronal connections. In: *Progress in Brain Research*, edited by M. Singer and J. P. Shade. Amsterdam: Elsevier, 1965, vol. 14, p. 1–32.

YUSTE, R. AND TANK, D. W. Dendritic integration in mammalian neurons, a century after Cajal. *Neuron* 16: 701–716, 1996.